Supporting Material

Area Per Lipid and Cholesterol Interactions in Membranes from Separated Local-Field ^{13}C NMR Spectroscopy

Avigdor Leftin[†,], Trivikram R. Molugu[†], Constantin Job[†], Klaus Beyer[†], and Michael F. Brown[†, ‡,*]

[†]Department of Chemistry and Biochemistry and [‡]Department of Physics, University of Arizona, Tucson, 85721, USA

Separated local-field NMR experiments: The NMR experiment DROSS (dipolar recoupling on-axis with scaling and shape preservation) (1) was implemented with the Bruker Topspin software platform (Billerica, MA). The timing diagram for the pulse sequence is shown in Fig. S1a. Magnetic dipolar recoupling during magic-angle spinning (MAS) is achieved by application of synchronous, phase-shifted recoupling π-pulse blocks (shown in Fig. S1b) during the indirect t_1 dimension. The module preserves the appearance of the Pake powder-pattern lineshapes due to the magnetic dipolar interaction. The conditions for the evolution of the second-rank Hamiltonian under MAS are not unique, and correspond to different values for the scaling of the anisotropic interactions χ_p and ε for the dipolar coupling and chemical shift anisotropy, respectively. For recoupling, we used the four-pulse module described by Tycko et al. (2). By applying symmetric recoupling pulses delivered at rotation angles of ± 70.9º, and ± 110.9º (shown in Fig. S1c), we achieved anisotropy scaling of χ_p = 0.393 and a chemical shift offset of ε = 0. The pulse sequence is sensitive to small errors in the rotor synchronization. Finite pulse widths and internal timing delays of the NMR spectrometer were accounted for in the pulse program. High-power radiofrequency amplifiers included a 1-kW

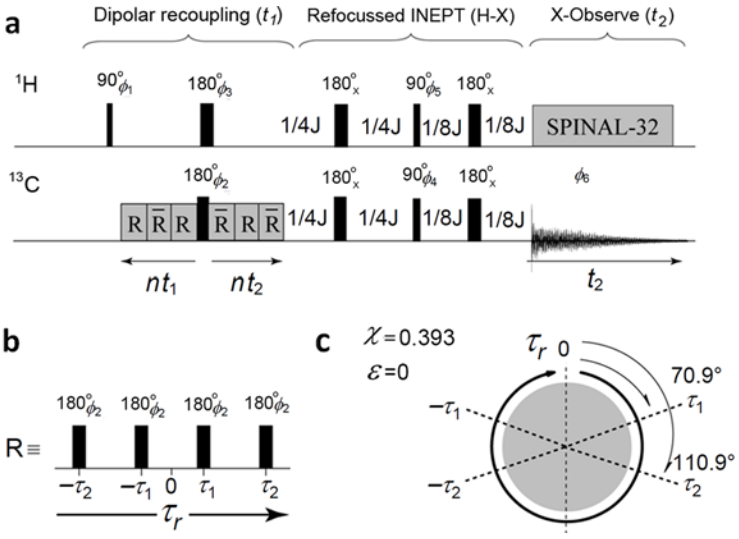

Fig. S1. Schematic representation of pulse sequence for DROSS experiment. (a) Timing diagram, (b) 4-pulse recoupling sequence, and (c) rotor synchronization timing with recoupling parameters χ=0.393 and ε=0.

low-frequency American Microwave Technologies (Lancaster, PA) amplifier and a 500-W high-frequency Tomco Technologies (Adelaide, Australia) amplifier. Radiofrequency pulses for the ^{1}H and ^{13}C channels were adjusted to exactly the same duration of 3.5 μs for the 90º pulses.

The refocused INEPT (insensitive nuclei enhanced by polarization transfer) method transfers dipolar-modulated ^{1}H magnetization to the directly-bound ^{13}C aliphatic nuclei for detection under ^{1}H decoupling using SPINAL-32 (3). The timing of the INEPT module in solution NMR requires $1/4J$ and $1/8J$ delays, with J being the average methylene ^{13}C–^{1}H scalar coupling of $J \approx$ 145 Hz. In the DROSS experiment, under MAS the rotor synchronization of the INEPT transfer, as well as any incompletely averaged dipolar couplings undergoing transverse precession during the polarization step, lead to optimal delays that differ from the solution NMR values. Maximum enhancement was ensured by monitoring the INEPT buildup of anti-phase magnetization and refocusing delays in a pseudo-2D array. For experiments conducted at 8-kHz MAS frequency, these delays were optimized to be 1.72 ms and 0.86 ms.

Two temperatures were chosen to conduct the DROSS experiments, 28 °C and 48 °C. These temperatures were selected based on the solid-ordered (s_o) to liquid-disordered (l_d) phase transition temperature of the EYSM lipid, which is reported to occur at approximately 38 ºC (4). This is an important aspect of our study, because for ^{13}H–^{13}C INEPT polarization transfer to efficiently occur, the components of the lipid membrane must be in the liquid-ordered, liquid-disordered, or isotropic phase (5). The refocused INEPT polarization transfer yields a null spectrum in the solid-ordered (s_o) phase. Hence, our comparisons of lipid mixtures are mostly discussed for results obtained at 48 °C. The behavior of binary membrane systems are qualitatively the same at both 28 ºC and 48 ºC, although magnitudes of the residual dipolar couplings (RDCs) are greater at the lower temperatures, and smaller chemical shift changes are obtained. Temperatures were calibrated to account for frictional and radiofrequency heating of the sample. Phase behavior of the lipids was also checked prior to the ^{13}C NMR experiments by collecting single-pulse ^{1}H NMR spectra. Temperatures reported are accurate to ± 1 ºC.

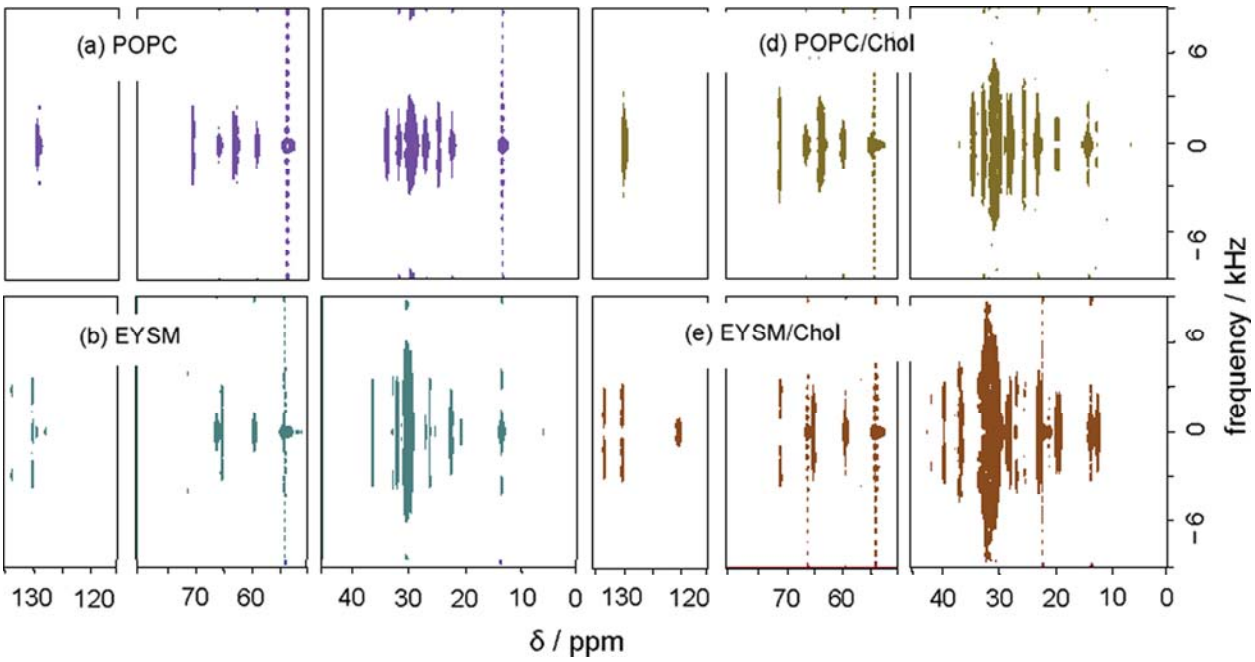

Fig. S2. Two-dimensional ^{13}C–^{1}H separated local-field contour plots for pure lipid bilayers and lipid/ cholesterol mixtures. The 2D planes obtained using the NMR experiment DROSS are shown for (a) POPC, (b) EYSM, (c) POPC/cholesterol (1:1), and (d) EYSM/cholesterol (1:1) lipid bilayers at 48 °C.

We conducted the 2D DROSS experiment for a series of membrane lipid systems to obtain the chemical shifts and RDCs for comparison with the raft-like system. Single-component POPC and EYSM membrane spectra were first collected. Then, the experiments were repeated for two-component POPC/cholesterol (1:1) and EYSM/cholesterol (1:1) bilayers to characterize the spectral behavior of the mixed systems. In Figs. S2a, b we show the separated-local field 2D spectra for the single-component POPC and EYSM membranes, respectively. Corresponding 2D spectra are shown in Figs. S2c, d for POPC/cholesterol (1:1) and EYSM/cholesterol (1:1) lipid mixtures at 48 °C. Isotropic ^{13}C chemical shifts and ^{13}C–^{1}H residual dipolar couplings for the single-component lipid membranes are presented in Fig. S3, and data for binary phospholipid/cholesterol systems in Fig. S4. The spectra demonstrate that the DROSS experiment is sensitive to changes in membrane phase, and that it is possible to extract site-specific ^{13}C chemical shifts and RDCs for individual lipids and lipid/cholesterol mixtures. The ^{13}C chemical shifts, measured ^{1}H–^{13}C residual dipolar couplings, and corresponding segmental order parameters are tabulated in Tables S1–Table S5 for all the samples studied.

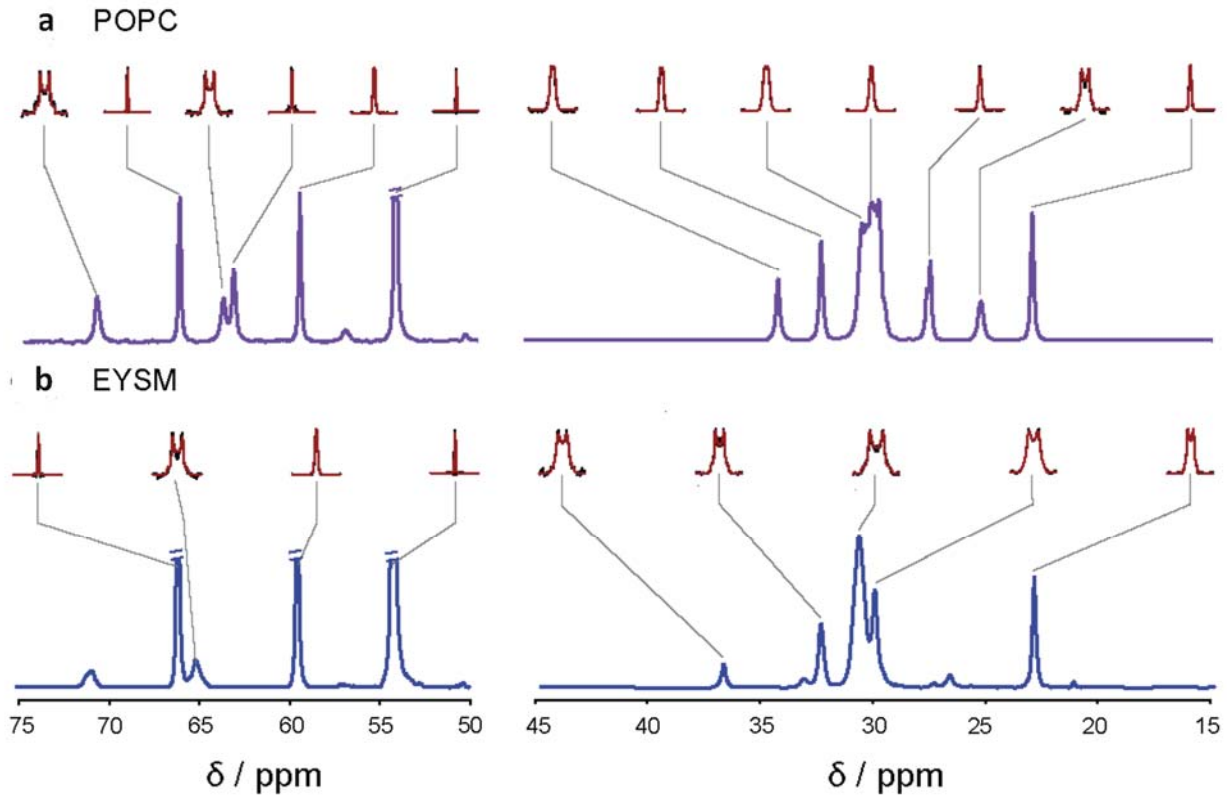

Fig. S3. Separated local-field NMR-derived ^{13}C chemical shifts and ^{13}C–^{1}H residual dipolar couplings (RDCs) for lipid bilayers. The slices along the F_1 (vertical) axis and projections onto the F_2 (horizontal) frequency axis of the 2D contour plots shown in Fig. S2 are indicated for (a) POPC and (b) EYSM (1:1) lipid bilayers at 48 °C.

Chemical shift assignments of solid-state ^{13}C lipid NMR spectra: The ^{13}C isotropic chemical shift spectra obtained under MAS were initially assigned using the literature values (6). However, chemical shift assignments for the region 29.5 ppm to 31.5 ppm are not available, where methylene resonances are significantly overlapping. Initially, we assigned this region using simulations (ChemBioDraw, PerkinElmer, MA) based on additive rules given for isotropic liquids (7-11). Such assignments gave expected results in the case of DMPC bilayers. The $|S_{CH}|$ order parameters were calculated for each chemical shift position and matched well with the $|S_{CD}|$ order parameters (12). For DMPC the ^{1}H–^{13}C dipolar order parameters calculated for the sites identified by such assignments are plotted against the corresponding quadrupolar order parameter values in Figs. S5 and S6 at 30 °C and 50 °C, respectively. For DMPC at 30 °C, a small discrepancy in the observed order parameters is seen for the *sn*-1 (Fig. S5a) and *sn*-2 (Fig. S5b) chains, but at 50 °C such a discrepancy is not seen (Figs. 6a, b).

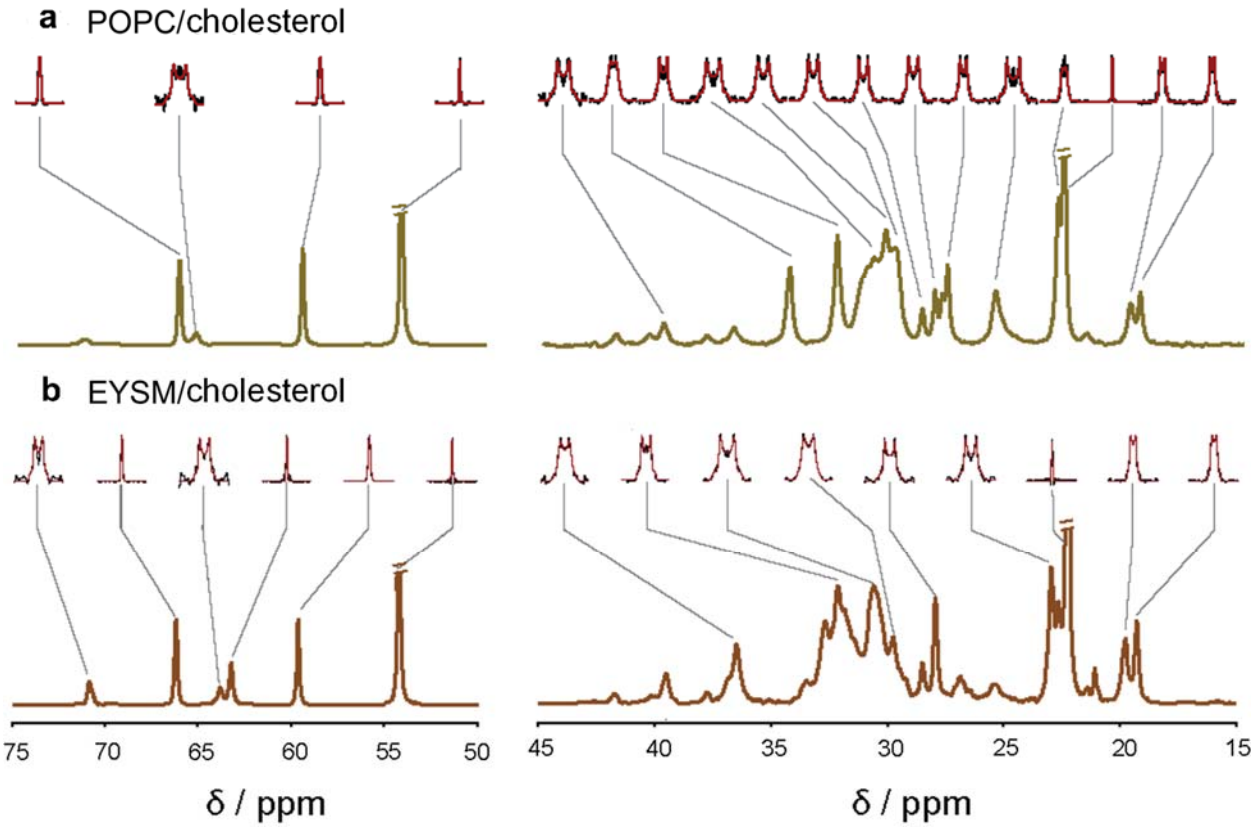

Fig. S4. Experimental ^{13}C chemical shifts and ^{13}C–^{1}H residual dipolar couplings (RDCs) for lipid/cholesterol mixtures. Slices along the F_1 axis (vertical) and F_2 (horizontal) projections of the 2D contour plots shown in Fig. S2 are indicated for (a) POPC/Chol (1:1) and (b) EYSM/Chol (1:1) lipid bilayers at 48 °C.

However, a similar strategy did not give the expected order parameter values in case of POPC bilayers (Figs. S7 and S8). The segmental $|S_{CH}|$ order parameters for unambiguously assigned chemical shift positions still matched with the known $|S_{CD}|$ order parameters (13) (shown as spheres in Figs. 7c, d). Yet the significant overlap of resonance peaks from the *sn*-1 palmitoyl chain and *sn*-2 oleoyl chain complicates the resonance assignments. The MAS-averaged chemical shift tensors of the less flexible acyl groups do not reach the isotropic chemical shift values. Instead they correspond to the chemical shift values due to tensorial averaging over the molecular conformations in the liquid-crystalline phase. At the spin rates employed here (6–8 kHz) MAS averages the residual chemical shielding tensor to its trace, which is not the same as averaging the static chemical shielding tensor. By contrast, in solution state NMR the isotropic chemical shifts are averaged over all possible conformations. Rapid molecular tumbling and rotational isomerizations about the chemical bonds average the static (so-called rigid-lattice) chemical shielding tensor to its isotropic value.

Consequently, we made use of the calculated $|S_{CH}|$ order parameter values at each resolved ^{13}C resonance peak as a basis to assign the ^{13}C chemical shift spectra in the crowded methylene (CH_2) spectral region. Initially the $|S_{CH}|$ order parameter values for all possible chemical shift positions were calculated. The order parameter values for well-defined peaks were then compared with the available $|S_{CD}|$ order parameters (12) at corresponding temperature values. For DMPC the $|S_{CH}|$ and $|S_{CD}|$ values consistently match, as shown by the unit slope in the $|S_{CD}|$ versus $|S_{CH}|$ plots in Figs. S5c, d and Figs. S6c, d. Next, we mapped the remaining calculated order parameters that were unassigned or ambiguously assigned with the known $|S_{CD}|$ order parameters, and fixed the chemical shift positions accordingly. A comparison of the ^2H NMR-assisted assignments and ChemBiodraw-based assignments for POPC bilayers at 28 °C are shown in Fig. S7 for the palmitoyl chain and Fig S8 for the oleoyl acyl chain. In this case the S_{CD}-assisted ^{13}C chemical shift assignments for the palmitoyl *sn*-1 chain (Figs. S7a, c) are in good agreement, whereas there is a significant discrepancy if the ChemBioDraw assignments are used (Figs. S7b, d). In the case of the oleoyl *sn*-2 chain of POPC, the S_{CD}-assisted ^{13}C NMR assignments give better agreement of the $|S_{CH}|$ and $|S_{CD}|$ order parameters (Figs. S8a, c) compared to ChemBioDraw assignments (Figs. S8b, d). Such an assignment strategy may not always apply to resonances that are not well resolved in solid-state ^2H NMR, and are treated as the plateau. Nonetheless, the application of ^2H NMR-assisted assignments is definitely useful for identifying the palmitoyl and oleoyl chains in the present case.

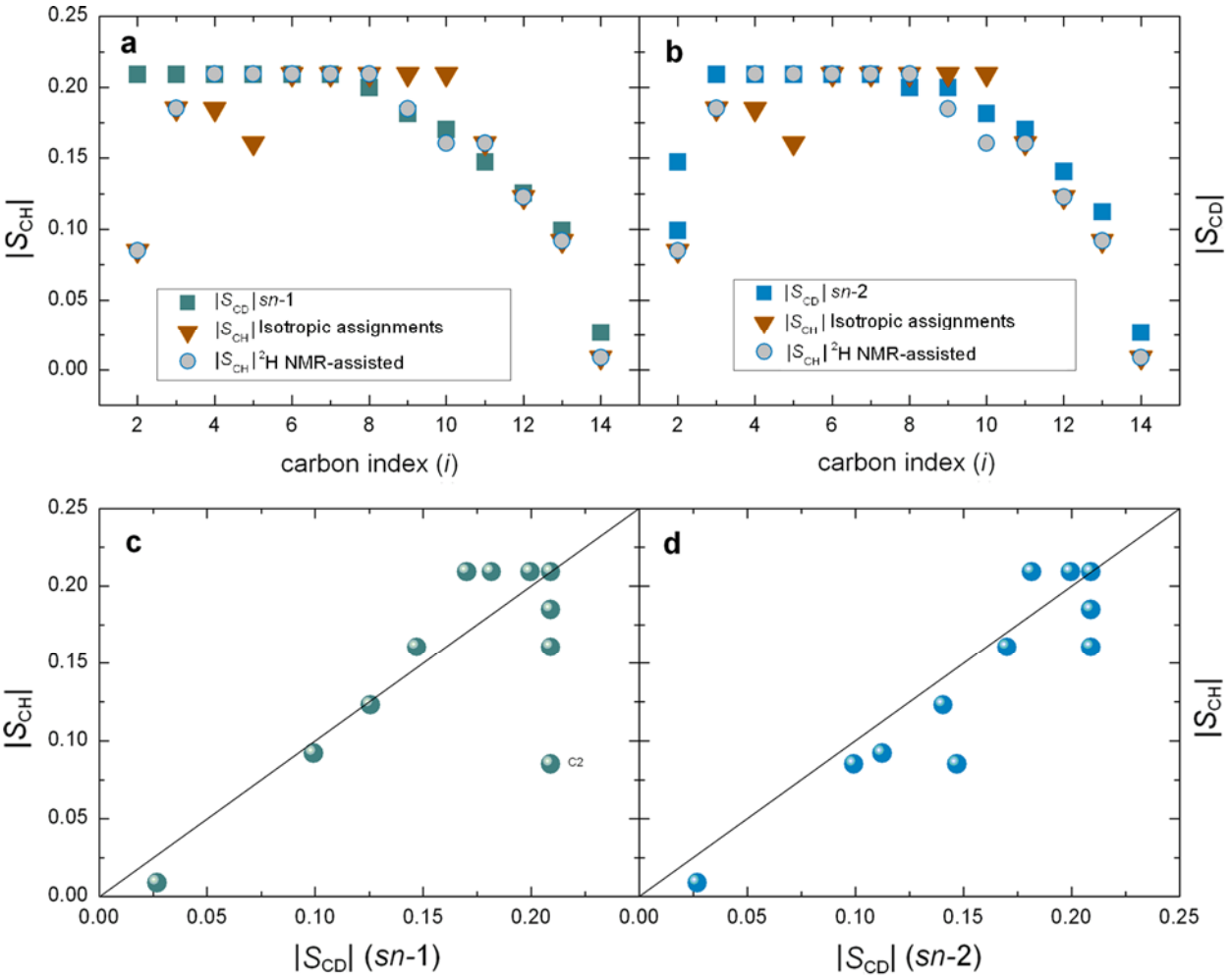

Fig. S5. Separated local-field ^{13}C NMR experiment provides $|S_{CH}|$ order parameters that correspond to $|S_{CD}|$ order parameters for DMPC bilayers in the liquid-crystalline (l_d) state at 30 °C. Absolute order parameters are plotted in terms of decreasing magnitudes as a function of peak (carbon) index (i): (a) $|S_{CD}|$ values (squares), $|S_{CH}|$ values with assignments based on additive rules for isotropic ^{13}C chemical shifts (triangles), and ^{2}H NMR-assisted (circles) order parameters as function of segmental carbon position of *sn*-1 chain. (b) $|S_{CD}|$ values (squares), $|S_{CH}|$ values with isotropic ^{13}C chemical shift assignments (triangles), and ^{2}H NMR-assisted order parameters (circles) as function of segmental carbon position for the *sn*-2 chain. Graphs of $|S_{CH}|$ order parameters from separated local-field ^{13}C NMR versus the corresponding $|S_{CD}|$ order parameters from solid-state ^{2}H NMR spectroscopy: (c) Plot of $|S_{CD}|$ order parameters versus ^{2}H NMR-assisted $|S_{CH}|$ order parameters for *sn*-1 chain. (d) Plot of $|S_{CD}|$ order parameters versus ^{2}H NMR-assisted $|S_{CH}|$ order parameters for *sn*-2 chain. Note that the $|S_{CH}|$ order parameters are in good agreement with the $|S_{CD}|$ values giving a near unit slope. Hence the ^{2}H NMR-derived $|S_{CD}|$ values can be used to guide ambiguous ^{13}C chemical shift assignments.

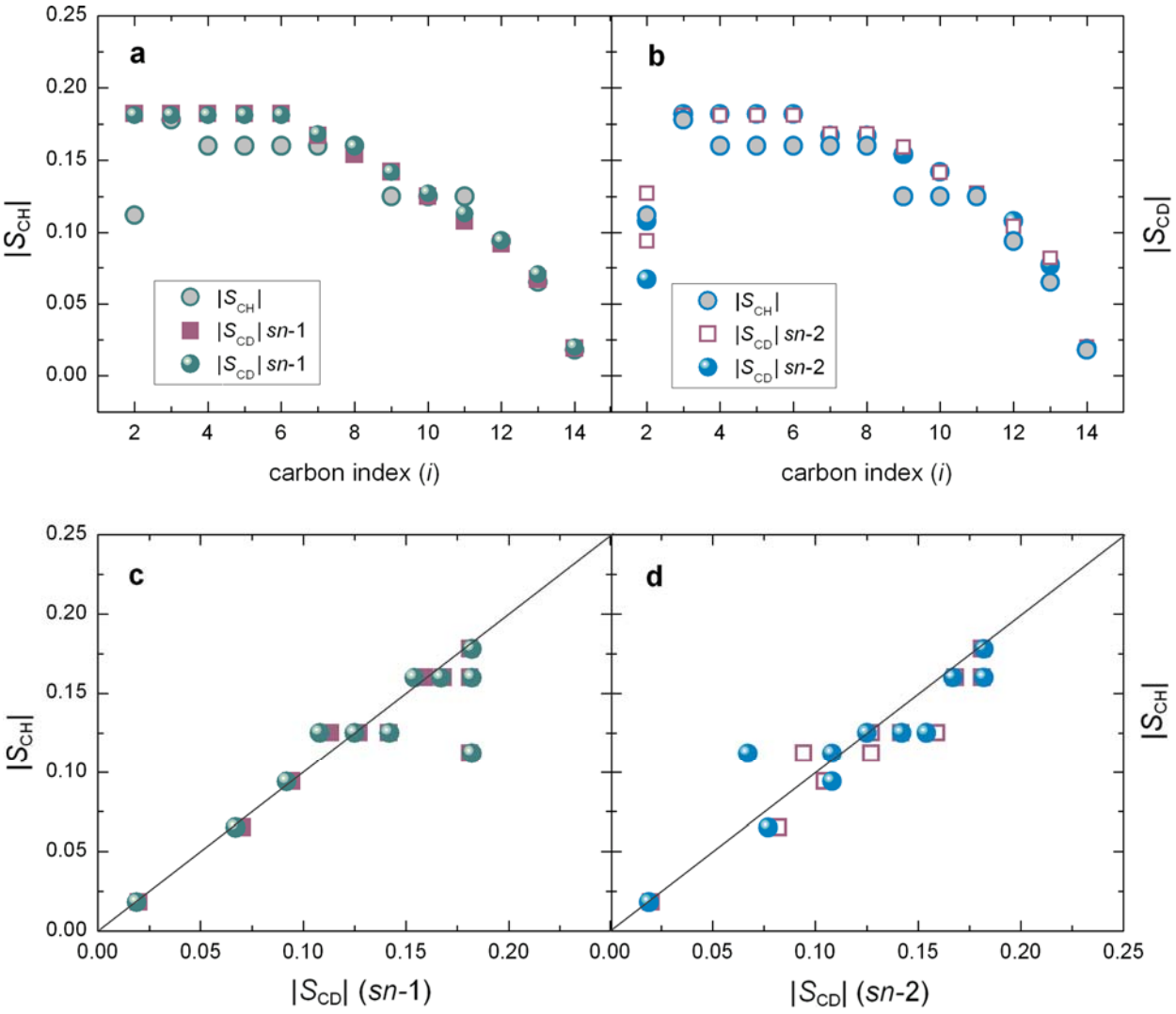

Fig. S6. Comparision of ^{13}C–^{1}H dipolar segmental order parameters $|S_{CH}|$ to corresponding $|S_{CD}|$ order parameters for DMPC bilayers at 50 °C. Absolute order parameters are plotted in terms of decreasing magnitudes as a function of peak (carbon) index (i): (a) $|S_{CH}|$ (grey circles) and $|S_{CD}|$ (spheres and squares) order parameters for *sn*-1 chain, (b) $|S_{CH}|$ (circles), and $|S_{CD}|$ (squares and spheres) order parameters as function of segmental carbon position in *sn*-2 chain. Separated-local field ^{13}C NMR order parameters $|S_{CH}|$ graphed against the $|S_{CD}|$ order parameters from solid-state ^{2}H NMR spectroscopy. (c) Plot of $|S_{CD}|$ order parameters versus $|S_{CH}|$ order parameters for *sn*-1 chain. (d) Plot of $|S_{CD}|$ order parameters versus $|S_{CH}|$ order parameters for *sn*-2 chain. The $|S_{CH}|$ order parameters are in good agreement with the $|S_{CD}|$ values giving a unit slope. In this example, the ^{2}H NMR-assisted method was not needed for ^{13}C chemical shift assignments.

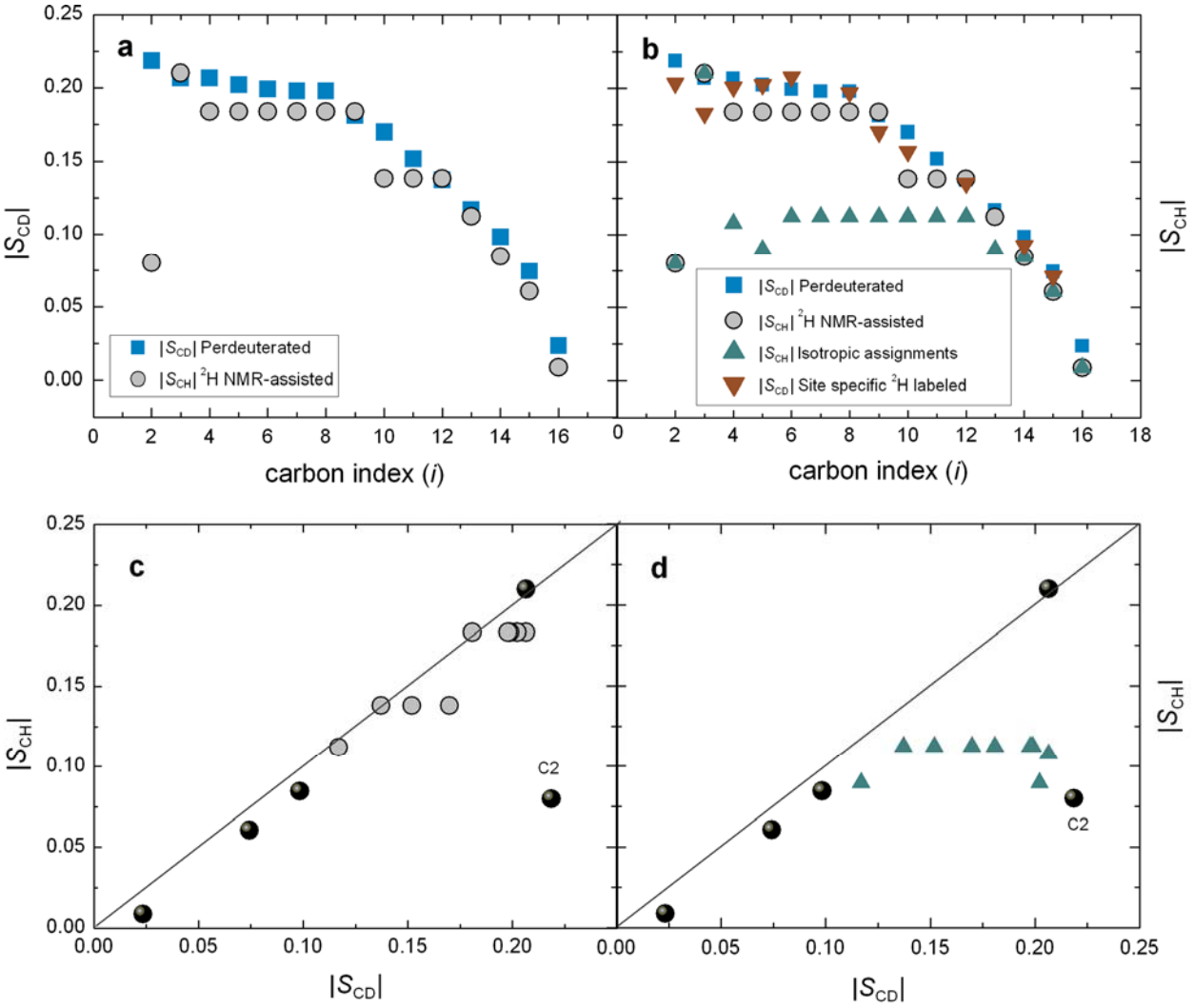

Fig. S7. Comparison of $|S_{CH}|$ order parameters from ^{13}C separated local-field NMR spectroscopy for the *sn*-1 palmitoyl chain of POPC to corresponding $|S_{CD}|$ values allows ^{2}H NMR-assisted chemical shift assignments. The applicability of such an assignment method is illustrated by comparing dipolar and quadrupolar order parameters for the liquid-crystalline (l_d) state of POPC bilayers at 28 °C. (a) The ^{2}H NMR-assisted $|S_{CH}|$ (circles) and $|S_{CD}|$ (squares) order parameters as function of segmental carbon position in the palmitoyl chain. (b) The $|S_{CD}|$ (squares) order parameters measured for the palmitoyl chain of POPC-d_{31} versus ^{2}H NMR-assisted $|S_{CH}|$ values (circles). Graph of the $|S_{CH}|$ order parameters from separated local-field ^{13}C NMR plotted against the corresponding solid-state ^{2}H NMR order parameters. (c) Segmental $|S_{CD}|$ order parameters versus ^{2}H NMR-assisted $|S_{CH}|$ order parameters. (d) $|S_{CD}|$ order parameters of perdeuterated palmitoyl group of POPC-d_{31} versus $|S_{CH}|$ order parameters obtained using isotropic ^{13}C chemical shift assignments. The $|S_{CH}|$ order parameters for all unambiguously assigned carbon positions (spheres in c and d) give a unit slope plotted against the corresponding $|S_{CD}|$ values. Note that ^{2}H NMR-derived $|S_{CD}|$ values can guide ambiguous ^{13}C resonance chemical shift assignments.*

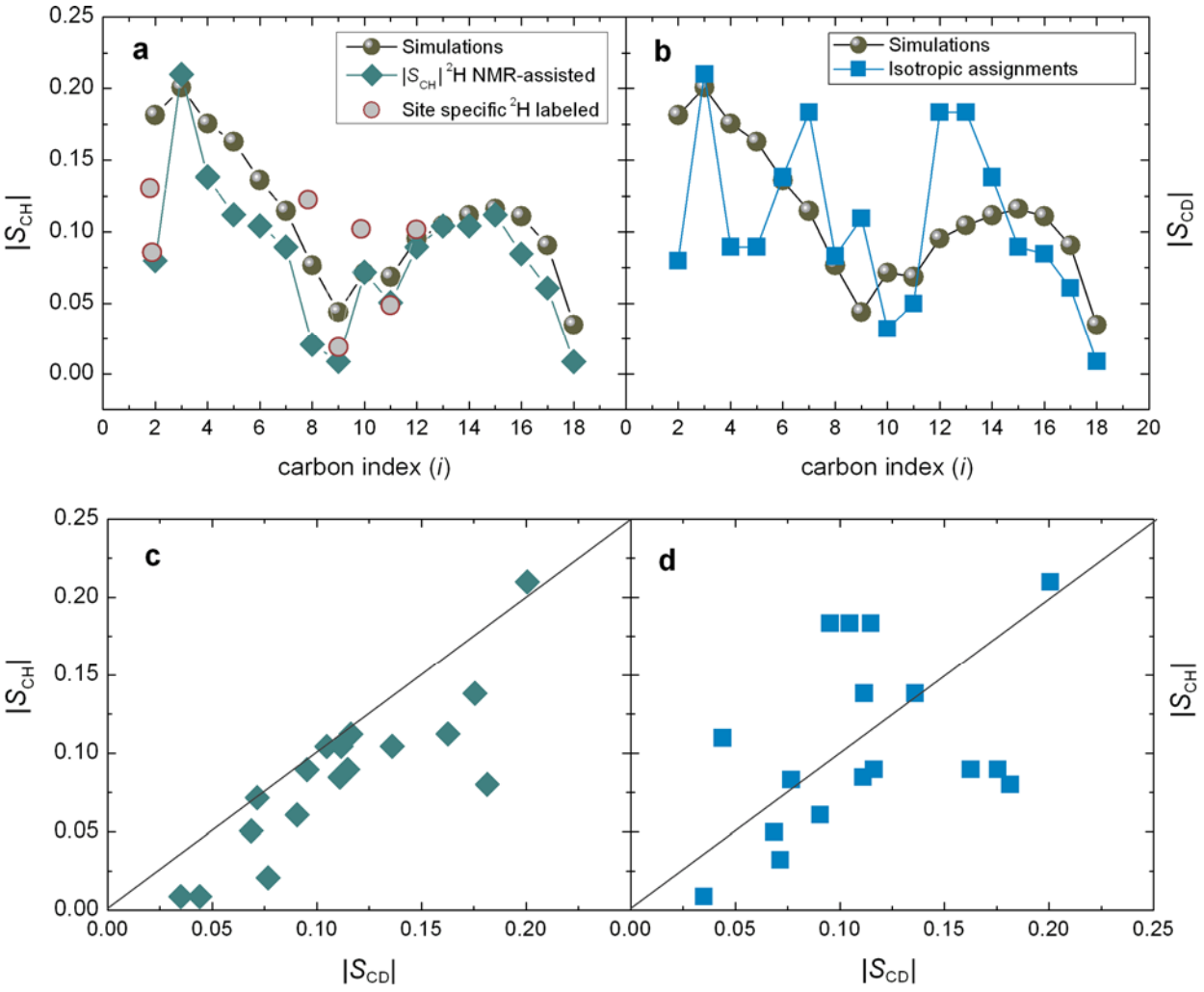

Fig. S8. Application of the $|S_{CD}|$-assisted ^{13}C chemical shift assignment method enables identification of *sn*-2 chain oleoyl resonances in the liquid-crystalline state of POPC at 28 °C. Comparison of $|S_{CH}|$ and $|S_{CD}|$ order parameters for the *sn*-2 oleoyl chain of the POPC lipid bilayer is shown. (a) The $|S_{CH}|$ order parameters with $|S_{CD}|$-assisted ^{13}C resonance assignments (diamonds), $|S_{CD}|$ order parameters (spheres) calculated using molecular dynamics simulations (13), and the $|S_{CD}|$ order parameters determined using ^{2}H-solid-state NMR for site specific deuterated lipid (grey filled circles). (b) The $|S_{CH}|$ order parameters (squares) calculated for *sn*-2 oleoyl chain of POPC with ^{13}C resonance assignments using additivity rules and $|S_{CD}|$ order parameters (spheres) calculated using molecular dynamics simulations. Plot of $|S_{CH}|$ order parameter from separated local-field ^{13}C NMR against the corresponding $|S_{CD}|$ order parameters: (c) Plot of the ^{2}H NMR-assisted $|S_{CH}|$ order parameters versus $|S_{CD}|$ order parameters. (d) The $|S_{CH}|$ order parameters calculated with ChemBioDraw assignments versus $|S_{CD}|$ order parameters.

Table S1. Summary of experimental results for DMPC bilayers

	Chemical Shift[a] / ppm		Dipolar Coupling[b] / Hz		Segmental Order Parameter[c]	
Resonance	30 ºC	50 ºC	30 ºC	50 ºC	30 ºC	50 ºC
C14	14.38	14.26	179.32	175.65	0.01	0.01
C13	23.3	23.15	1422.60	1353.61	0.09	0.08
C12	32.73	32.55	2559.80	1923.66	0.12	0.07
C11	30.32	30.09	3450.38	2541.98	0.12	0.13
C10	30.32	30.59	3450.38	2541.98	0.16	0.13
C9	30.32	30.09	3450.38	2541.98	0.19	0.13
C8	30.87	30.59	3382.19	257500	0.21	0.16
C7	30.87	30.59	3382.19	2575.00	0.21	0.16
C6	30.87	30.59	3382.19	3257.00	0.21	0.16
C5	30.87	30.59	3382.19	2575.00	0.21	0.16
C4	30.32	30.09	3250.38	2541.98	0.21	0.16
C3	30.87	30.59	3982.19	3257.00	0.19	0.18
C2	25.67	25.49	4218.83	3628.5	0.09	0.12
sn-1	64.29	64.24	4920.10	4501.27	0.31	0.29
sn-2	71.33	71.34	2270.74	2064.76	0.14	0.13
sn-3	63.71	63.66	363.87	363.87	0.02	0.02
α	60.11	60.04	280.48	250.53	0.02	0.02
β	66.71	66.73	516.15	368.63	0.03	0.02
γ	54.74	54.74	180.33	200.02	0.01	0.01

[a]Chemical shifts are referenced to TMS (external).

[b]Dipolar couplings are scaled by the pulse sequence scale factor χ_p=0.393.

[c]Absolute value.

Table S2. Summary of experimental results for POPC bilayers

	Chemical Shift[a] / ppm				Dipolar Coupling[b] / Hz				Segmental Order Parameter[c]			
	Palmitoyl		Oleoyl		Palmitoyl		Oleoyl		Palmitoyl		Oleoyl	
Resonance	28 ºC	48 ºC	28 ºC	48 ºC	28 ºC	48 ºC	28 ºC	48 ºC	28 ºC	48 ºC	28 ºC	48 ºC
C18	--	--	13.84	13.78	--	--	323	300	--	--	0.01	0.01
C17	--	--	22.67	22.60	--	--	758	486	--	--	0.06	0.04
C16	13.84	13.78	32.04	31.96	323	300	1120	896	0.01	0.01	0.09	0.07
C15	22.67	22.60	29.75	29.63	758	486	1573	967	0.06	0.04	0.11	0.07
C14	32.04	31.96	29.88	29.82	1120	896	1753	1611	0.09	0.07	0.10	0.07
C13	29.75	29.63	29.88	29.82	1573	967	1753	1611	0.11	0.07	0.10	0.07
C12	29.88	29.82	29.88	29.82	1753	1611	1753	1611	0.14	0.11	0.09	0.08
C11	29.88	29.82	27.25	27.21	1753	1611	725	364	0.14	0.11	0.05	0.04
C10	30.21	30.06	129.34	129.35	1753	1611	486	244	0.18	0.16	0.07	0.06
C9	30.21	30.06	129.72	129.71	1753	1611	1448	1265	0.18	0.16	0.01	0.01
C8	30.21	30.06	27.25	27.21	1753	1611	725	364	0.18	0.16	0.02	0.07
C7	30.21	30.06	29.88	29.82	1753	1611	1753	1611	0.18	0.16	0.09	0.08
C6	30.21	30.06	29.88	29.82	1753	1611	1753	1611	0.18	0.16	0.10	0.07
C5	30.21	30.06	29.75	29.63	1573	967	1573	967	0.18	0.16	0.11	0.07
C4	30.21	30.06	29.47	29.37	1282	364	1282	364	0.18	0.16	0.14	0.08
C3	25.02	24.98	25.02	24.98	2802	2651	2802	2651	0.21	0.18	0.21	0.18
C2	34.07	34.07	34.07	34.07	1552	1448	1552	1448	0.08	0.08	0.08	0.07
sn-1	63.09	63.10	63.09	63.10	244	244	244	244	0.02	0.02	0.02	0.02
sn-2	70.73	70.80	70.73	70.80	2949	2893	2949	2893	0.19	0.18	0.19	0.18
sn-3	63.68	63.66	63.68	63.66	3394	3539	3394	3539	0.21	0.22	0.21	0.22
α	59.50	59.49	59.50	59.49	486	486	486	486	0.03	0.03	0.03	0.03
β	66.11	66.19	66.11	66.19	486	244	486	244	0.03	0.02	0.03	0.02
γ	54.13	54.19	54.13	54.19	303	244	303	244	0.02	0.02	0.02	0.02

[a]Chemical shifts are referenced to TMS (external).

[b]Dipolar couplings are scaled by the pulse sequence scale factor χ_p=0.393.

[c]Absolute value.

Table S3. Summary of experimental results for EYSM bilayers

	Chemical Shift[a] / ppm				Dipolar Coupling[b] / Hz				Segmental Order Parameter[c]			
	Sphingosine		Fatty Acyl		Sphingosine		Fatty Acyl		Sphingosine		Fatty Acyl	
Resonance	28 ºC	48 ºC	28 ºC	48 ºC	28 ºC	48 ºC	28 ºC	48 ºC	28 ºC	48 ºC	28 ºC	48 ºC
C16	--	--	--	14.10	--	--	--	282	--	--	--	0.014
C15	--	--	--	23.07	--	--	--	2249	--	--	--	0.110
S18 / C14	--	14.10	--	32.54	--	282	--	3204	--	0.014	--	0.157
S17 / C13	--	23.07	--	30.15	--	2249	--	3931	--	0.110	--	0.193
S16 / C12	--	32.54	--	30.85	--	3204	--	5064	--	0.157	--	0.248
S15 / C11	--	30.15	--	30.85	--	3931	--	5064	--	0.193	--	0.248
S14 / C10	--	30.85	--	30.85	--	5064	--	5064	--	0.248	--	0.248
S13 / C9	--	30.85	--	30.85	--	5064	--	5064	--	0.248	--	0.248
S12 / C8	--	30.85	--	30.85	--	5064	--	5064	--	0.248	--	0.248
S11 / C7	--	30.85	--	30.85	--	5064	--	5064	--	0.248	--	0.248
S10 / C6	--	30.85	--	30.85	--	5064	--	5064	--	0.248	--	0.248
S9 / C5	--	30.85	--	30.85	--	5064	--	5064	--	0.248	--	0.248
S8 / C4	--	30.85	--	30.15	--	5064	--	3931	--	0.248	--	0.193
S7 / C3	--	30.85	--	26.81	--	5064	--	--	--	0.248	--	--
S6 / C2	--	30.15	--	36.86	--	3931	--	3649	--	0.193	--	0.179
S5	--	134.09	--	--	--	5539	--	--	--	0.272	--	--
S4	--	130.44	--	--	--	5664	--	--	--	0.278	--	--
S3	--	71.57	--	--	--	6837	--	--	--	0.335	--	--
S2	--	--	--	--	--	--	--	--	--	--	--	--
S1	--	65.59	--	65.59	--	4677	--	4677	--	0.229	--	0.229
α	--	59.87	--	59.87	--	282	--	282	--	0.014	--	0.014
β	--	66.48	--	66.48	--	282	--	282	--	0.014	--	0.014
γ	--	54.56	--	54.56	--	282	--	282	--	0.014	--	0.014

[a]Chemical shifts are referenced to TMS (external).

[b]Dipolar couplings are scaled by the pulse sequence scale factor $\chi_p = 0.393$.

[c]Absolute values.

Table S4. Summary of experimental results for POPC/Chol (1:1) bilayers

	Chemical Shift[a] / ppm				Dipolar Coupling[b] / Hz				Segmental Order Parameter[c]			
	Palmitoyl		Oleoyl		Palmitoyl		Oleoyl		Palmitoyl		Oleoyl	
Resonance	28 ºC	48 ºC	28 ºC	48 ºC	28 ºC	48 ºC	28 ºC	48 ºC	28 ºC	48 ºC	28 ºC	48 ºC
C18	--	--	14.12	14.01	--	--	1274	317	--	--	0.08	0.02
C17	--	--	28.57	22.88	--	--	2784	2321	--	--	0.18	0.15
C16	14.12	14.01	32.56	32.41	779	176	4252	3880	0.08	0.02	0.28	0.25
C15	23.02	22.88	30.08	29.93	2753	2321	5237	4845	0.18	0.15	0.34	0.32
C14	32.56	32.41	30.46	30.31	4252	3880	5758	5588	0.28	0.25	0.38	0.37
C13	30.08	29.93	30.46	30.31	5237	4845	5758	5588	0.34	0.32	0.38	0.37
C12	30.46	30.31	31.07	30.82	7262	6768	5758	5588	0.47	0.44	0.38	0.37
C11	30.46	30.31	31.07	30.82	7262	6768	3422	3323	0.47	0.44	0.22	0.22
C10	30.46	30.31	31.07	30.82	7262	6768	2235	2051	0.47	0.44	0.14	0.13
C9	30.46	30.31	31.07	30.82	7262	6768	842	794	0.47	0.44	0.05	0.05
C8	30.46	30.31	31.07	30.82	7262	6768	4669	4344	0.47	0.44	0.31	0.28
C7	30.46	30.31	31.07	30.82	7262	6768	7262	6768	0.47	0.44	0.38	0.37
C6	30.46	30.31	31.07	30.82	7262	6768	5758	5588	0.47	0.44	0.38	0.37
C5	30.46	30.31	31.07	30.82	7262	6768	5237	4845	0.47	0.44	0.34	0.32
C4	30.08	29.93	30.08	29.93	5237	4845	5237	4845	0.34	0.32	0.34	0.32
C3	25.72	25.58	25.72	25.58	6450	6122	6450	6122	0.42	0.40	0.42	0.40
C2	34.50	34.45	34.50	34.45	3608	3537	3608	3537	0.24	0.23	0.24	0.23
sn-1	63.49	63.45	63.49	63.45	349	349	349	349	0.02	0.02	0.02	0.02
sn-2	71.01	71.04	71.01	71.04	4835	4539	4835	4539	0.30	0.29	0.16	0.15
sn-3	64.06	64.01	64.06	64.01	4201	4206	4201	4206	0.27	0.28	0.27	0.28
α	59.84	59.78	59.84	59.78	176	959	176	959	0.01	0.06	0.01	0.06
β	66.41	66.45	66.41	66.45	349	349	349	349	0.02	0.02	0.02	0.02
γ	54.45	54.47	54.45	54.47	344	349	344	349	0.03	0.03	0.03	0.03

[a]Chemical shifts are referenced to TMS (external).

[b]Dipolar couplings are scaled by the pulse sequence scale factor $\chi_p = 0.393$.

[c]Absolute values.

Table S5. Summary of experimental results for EYSM/Chol (1:1) bilayers

	Chemical Shift[a] / ppm				Dipolar Coupling[b] / Hz				Segmental Order Parameter[c]			
	Sphingosine		Fatty Acyl		Sphingosine		Fatty Acyl		Sphingosine		Fatty Acyl	
Resonance	28 ºC	48 ºC	28 ºC	48 ºC	28 ºC	48 ºC	28 ºC	48 ºC	28 ºC	48 ºC	28 ºC	48 ºC
C16	--	--	13.81	13.74	--	--	1041	919	--	--	0.051	0.045
C15	--	--	23.06	22.95	--	--	4092	3761	--	--	0.201	0.184
S18 / C14	13.81	13.74	32.80	32.66	1041	919	6491	5771	0.051	0.045	0.318	0.283
S17 / C13	23.06	22.95	30.84	30.64	4092	3761	6975	6265	0.201	0.184	0.341	0.307
S16 / C12	32.80	32.66	30.84	30.64	6491	5771	6975	6265	0.318	0.283	0.341	0.307
S15 / C11	30.84	30.64	30.84	30.64	6975	6265	6975	6265	0.341	0.307	0.341	0.307
S14 / C10	30.84	30.64	30.84	30.64	6975	6265	6975	6265	0.341	0.307	0.341	0.307
S13 / C9	30.84	30.64	30.84	30.64	6975	6265	6975	6265	0.341	0.307	0.341	0.307
S12 / C8	30.84	30.64	30.84	30.64	6975	6265	6975	6265	0.341	0.307	0.341	0.307
S11 / C7	30.84	30.64	30.84	30.64	6975	6265	6975	6265	0.341	0.307	0.341	0.307
S10 / C6	30.84	30.64	30.84	30.64	6975	6265	6975	6265	0.341	0.307	0.341	0.307
S9 / C5	30.84	30.64	30.84	30.64	6975	6265	6975	6265	0.341	0.307	0.341	0.307
S8 / C4	30.84	30.64	30.84	30.64	6975	6265	6975	6265	0.341	0.307	0.341	0.307
S7 / C3	30.84	30.64	26.97	26.86	6975	6265	--	--	0.341	0.307	--	--
S6 / C2	30.84	30.64	37.03	36.53	6975	6265	--	2687	0.341	0.307	--	0.132
S5	133.59	133.54	133.59	133.54	--	4692	--	4692	--	0.230	--	0.230
S4	130.28	130.31	130.28	130.31	--	4819	--	4819	--	0.236	--	0.236
S3	70.94	70.96	70.94	70.96	5527	5779	5527	5779	0.271	0.283	0.271	0.283
S2	--	--	--	--	--	--	--	--	--	--	--	--
S1	65.09	65.14	65.09	65.14	3705	3550	3705	3550	0.182	0.174	0.182	0.174
α	59.51	59.51	59.51	59.51	244	364	244	364	0.012	0.018	0.012	0.018
β	66.11	66.17	66.11	66.17	318	280	318	280	0.016	0.014	0.016	0.014
γ	54.16	54.22	54.16	54.22	305	244	305	244	0.015	0.012	0.015	0.012

[a]Chemical shifts are referenced to TMS (external).

[b]Dipolar couplings are scaled by the pulse sequence scale factor χ_p=0.393.

[c]Absolute values.

Supporting References

1. Gross, J. D., D. E. Warschawski, and R. G. Griffin. 1997. Dipolar recoupling in MAS NMR: a probe for segmental order in lipid bilayers. *J. Am. Chem. Soc.* 119:796-802.
2. Tycko, R., G. Dabbagh, and P. A. Mirau. 1989. Determination of chemical shift anisotropy lineshapes in a two dimensional magic angle spinning NMR experiment. *J. Magn. Reson.* 85:265-274.
3. Fung, B. M., A. K. Khitrin, and K. Ermolaev. 2000. An improved broadband decoupling sequence for liquid crystals and solids. *J. Magn. Reson.* 142:97-101.
4. Shipley, G. G., L. S. Avecilla, and D. M. Small. 1974. Phase behaviour and structure of aqueous dispersions of sphingomyelin. *J. Lipid Res.* 15:124.
5. Warschawski, D. E., and P. F. Deveaux. 2005. Order parameters of unsaturated phospholipids in membranes and the effect of cholesterol: a ^{1}H-^{13}C solid-state NMR study at natural abundance. *Eur. Biophys. J.* 34:987-996.
6. Volke, F., R. Waschipky, A. Pampel, A. Donnerstag, G. Lantzsch, H. Pfeiffer, W. Richter, G. Klose, and P. Welzel. 1997. Characterisation of antibiotic moenomycin A interaction with phospholipid model membranes. *Chem. Phys. Lipids* 85:115-123.
7. Fürst, A., and E. Pretsch. 1990. A computer program for the prediction of ^{13}C-NMR chemical shifts of organic compounds. *Anal. Chim. Acta* 229:17-25.
8. Pretsch, E., A. Fürst, M. Badertscher, R. Bürgin, and M. E. Munk. 1992. C13shift: a computer program for the prediction of ^{13}C NMR spectra based on an open set of additivity rules. *J. Chem. Inf. Comput. Sci.* 32:291-295.
9. Schaller, R. B., C. Arnold, and E. Pretsch. 1995. New parameters for predicting ^{1}H-NMR chemical-shifts of protons attached to carbon-atoms. *Anal. Chim. Acta* 312:95-105.
10. Schaller, R. B., M. E. Munk, and E. Pretsch. 1996. Spectra estimation for computer-aided structure determination. *J. Chem. Inf. Comput. Sci.* 36:239-243.
11. Schaller, R. B., and E. Pretsch. 1994. A computer-program for the automatic estimation of ^{1}H-NMR chemical-shifts. *Anal. Chim. Acta* 290:295-302.
12. Leftin, A., and M. F. Brown. 2011. An NMR database for simulations of membrane dynamics. *Biochim. Biophys. Acta* 1808:818-839.
13. Huber, T., K. Rajamoorthi, V. F. Kurze, K. Beyer, and M. F. Brown. 2002. Structure of docosahexaenoic acid-containing phospholipid bilayers as studied by ^{2}H NMR and molecular dynamics simulations. *J. Am. Chem. Soc.* 124:298-309.